Artemisinin Derivatives with Antimalarial Activity against *Plasmodium falciparum* Designed with the Aid of Quantum Chemical and Partial Least Squares Methods

José C. Pinheiro*, Rudolf Kiralj, Márcia M. C. Ferreira**

Laboratório de Quimiometria Teórica e Aplicada, Instituto de Química, Universidade Estadual de Campinas, 13083-974 Campinas, SP, Brazil

Oscar A. S. Romero

Departamento de Química, Centro de Ciências Exatas e Naturais, Universidade Federal do Pará, 66075-110 Belém, PA, Brazil

Full Paper

Artemisinin derivatives with antimalarial activity against ***Plasmodium falciparum*** resistant to mefloquine are designed with the aid of Quantum Chemical and Partial Least Squares Methods. The PLS model with three principal components explaining 89.55% of total variance, $Q^2 = 0.83$ and $R^2 = 0.92$ was obtained for 14/5 molecules in the training/external validation set. The most important descriptors for the design of the model were one level above the lowest unoccupied molecular orbital energy (LUMO + 1), atomic charges in atoms C9 and C11 (Q_9) and (Q_{11}) respectively, the maximum number of hydrogen atoms that might make contact with heme (NH) and RDF030 m (a radial distribution function centered at 3.0 Å interatomic distance and weighted by atomic masses). From a set of ten proposed artemisinin derivatives, a new compound (**26**), was predicted with antimalarial activity higher than the compounds reported in literature. Molecular graphics and modeling supported the PLS results and revealed heme-ligand and protein-ligand stereoelectronic relationships as important for antimalarial activity. The most active **26** and **29** in the prediction set possess substituents at C9 able to extend to hemoglobin exterior, what determines the high activity of these compounds.

1 Introduction

Malaria has been known since ancient times. Hippocratic in his writings had already mentioned different manifestations of that disease as the enlargement of the spleen [1]. At the present time, some 40% of the world's population is exposed to the risk of contracting malaria, and that every year about 2.7 million people die in consequence of that disease. There are four members of the ***Plasmodium*** gender that infect humans and all are transmitted through the bite of the Anofeles female mosquito. Most of the deaths are attributed to the parasite species ***falciparum***. The severity of the disease caused by this species results primarily from its ability to modify the surface of infected red blood cells by inserting parasite proteins [2]. The enzymes in parasite digestive vacuole (cysteine and aspartic proteinases) break down hemoglobin into amino-acids and heme [3]. While all amino-acid contents is used for building parasite proteins, only a small portion of heme is incorporated into parasite hemoproteins; the rest of heme is detoxified (polymerized) caused by parasite enzymes [4]. A number of drugs have been investigated for their efficacy in the treatment of malaria [5], however, the appearance of resistant strains of ***falciparum*** to some of those drugs has made necessary further investigation of new classes of compounds which might have effective action against them [6–10]. Also, computational [5, 11–13] and quantitative structure-activity relationship (QSAR) studies [6, 8, 14–18] of any of those

* *Permanent address: Laboratório de Química Teórica e Computacional, Centro de Ciências Exatas e Naturais, Universidade Federal do Pará, 66075-110 Belém, PA, Brasil*

** Corresponding author: Laboratório de Quimiometria Teórica e Aplicada, Instituto de Química, Universidade Estadual de Campinas, 13081-970 Campinas, SP, Brasil; E-mail: marcia@iqm.unicamp.br; Phone: +55 19 3788 3102; Fax: +55 19 3788 3023

Key words: Artemisinin derivatives, Antimalarial activity, ***Plasmodium falciparum***, Quantum Chemical Methods, PLS, QSAR, Molecular Graphics and Modeling

 © 2003 WILEY-VCH Verlag GmbH & Co. KGaA, Weinheim

drugs have been done aiming to unravel its mechanisms of action and guidelines for the syntheses of new derivatives with improved efficiency.

Among the classes of drugs that are effective in the clinical treatment of the ***falciparum*** malaria, there is the artemisinin or *qinghaosu* and its derivatives. Artemisinin was originally extracted from the herb *Artemisia annua* or *qinghao* and used for the treatment of 52 kind of diseases in China [1, 19]. It is not known yet which is the true mechanism of artemisinin antimalarial activity. Various experimental and theoretical studies suggest existence of several processes involving artemisinin, as inhibition of heme polymerization, breaking hemozoin into heme units or damaging the parasite membrane [4]. The first step of artemisinin action includes heme-catalyzed artemisinin activation into a very reactive radical, and the next covalent binding of the radical to parasite proteins or heme [4], hemozoin [20], reduced glutathione [21] or other parasite molecules.

In this work, Quantum Chemical and Partial Least Squares methods are employed in the design of the Artemisinin derivatives with antimalarial activity against ***Plasmodium flaciparum***. Molecular graphics and modeling study on artemisinine-heme binding mode, also employing experimental ligand-heme structures, is performed as an additional methodology companion to the PLS study. Docking of atemisinin and some derivatives to hemoglobin A is carried out and a new view on artemisinin-heme binding is proposed. Artemisinin activation seems to be a crucial point in its antimalarial activity [22], what justifies the study of artemisinin-heme binding before the activation. The compounds shown in Figure 1 [23, 24] are initially studied with the Hartree-Fock (HF)/6–31G* method [25, 26]. Partial Least Squares (PLS) [27, 28] method is then used to build a multivariate regression model and predict the unknown antimalarial activity of the new Artemisinin derivatives shown in Figure 2.

2 Methodology

2.1 Geometry Optimization and Calculation of Molecular Descriptors

The compounds in Fig. 1 were tested *in vivo* against the human malaria ***Plasmodium falciparum*** Sierra Leone clone D-6 resistant to mefloquine [23, 24, 29]. All the activities used in this work were logarithms of IC_{50} relative to artemisinin ($\log IC_{50}$). As the activities were measured under three different conditions, the activities for **13–19** [24, 29] were rescaled with respect to activities for **1–12** [23] by using $\log IC_{50}$ for compounds obtained from two experiments. All the compounds (Figs. 1 and 2) were modeled using GaussView program [30] and complete geometry optimization with the *ab initio* HF/6–31G* method was performed. The structures obtained by *ab initio* method using different basis sets [12, 18] were compared with those determined by X-ray crystallography [31, 32] (retrieved from the Cambridge Structural Database CSD [33] with REFCODES: QNGHSU10 [31] and QNGHSU03 [32], crystallographic *R* factor 5.72% and 3.60%, respectively). In Protein Data Bank (PDB) [34] there are no artemisinin containing experimental structures nor theoretical models. Table 1 shows the experimental and calculated parameters of artemisinin 1,2,4-trioxane ring. It can be seen that the bond lengths are well described by all calculations performed. Also, all calculated bond angles are nearly close to the obtained experimental values. The torsion angles of the twist boat conformation adopted in the artemisinin shows very good agreement between the HF/6–31G* [12], HF/6–31G [18], HF/6–31G* (this work), and the experimental values [31, 32].

Quantum chemical descriptors calculation was carried out using Gaussian 98 program and the DIRECT-SCF method [35] in the conformation that is the most stable for a given compound. The atom numbering adopted in Figure 1 (compound **1**) is the same utilized by Acton *et* al. [23, 24]. The oxygen atom at C10, is numbered as O10 and the three methyl groups in C3, C6 and C9 are referred as 3-Me, 6-Me and 9-Me, respectively. Quantum-chemical descriptors were calculated, as for example: molecular HOMO, HOMO−1, LUMO and LUMO+1 energies, HOMO – LUMO gap, Mulliken's electronegativity, molecular hardness and softness, dipole moment, atomic charges on Nth atom (Q_N, N = 1 to 15); O1–C2 bond length, C–O–O–C torsion angle. The atomic charges used in this work were obtained with the CHELPG keyword through the electrostatic potential [36]. Also, the maximum number of hydrogen atoms (NH) that can interact with the heme is used in this work. It was generated from 2D structures, based on chemical knowledge of organic stereochemistry. This descriptor describes the hydrophobic part of artemisinin, as the maximum number of hydrogen atoms that could theoretically participate in the C–H ... π (heme) interactions. All axial hydrogen atoms (5a, 8a, 4, 7, 9), one hydrogen from each methyl group (3-Me, 6-Me, 9-Me), and a certain number of hydrogens from substituents at C9 (those which would satisfy the geometrical conditions for C–H ... π interactions) were counted. Furthermore, molecular descriptors implemented in the Dragon program [37, 38], were calculated, as for example radial distribution function – centered at 3.0 Å interatomic distances and weighted by atomic masses (RDF030 m) [39]. Some physicochemical descriptors were included also, as for example: the polar surface area, molecular volume, molecular refractivity and polarizability, logarithm of the octanol-water partition coefficient, molecular mass. They were calculated using the ChemPlus module [40] and Dragon program.

From all the descriptors above mentioned, it can be considered that some of them give valuable information about the influence of electronic, steric, and or hydrophobic features upon the biological activity of drug molecules. In this work, the molecular descriptors were selected so that

© 2003 WILEY-VCH Verlag GmbH & Co. KGaA, Weinheim

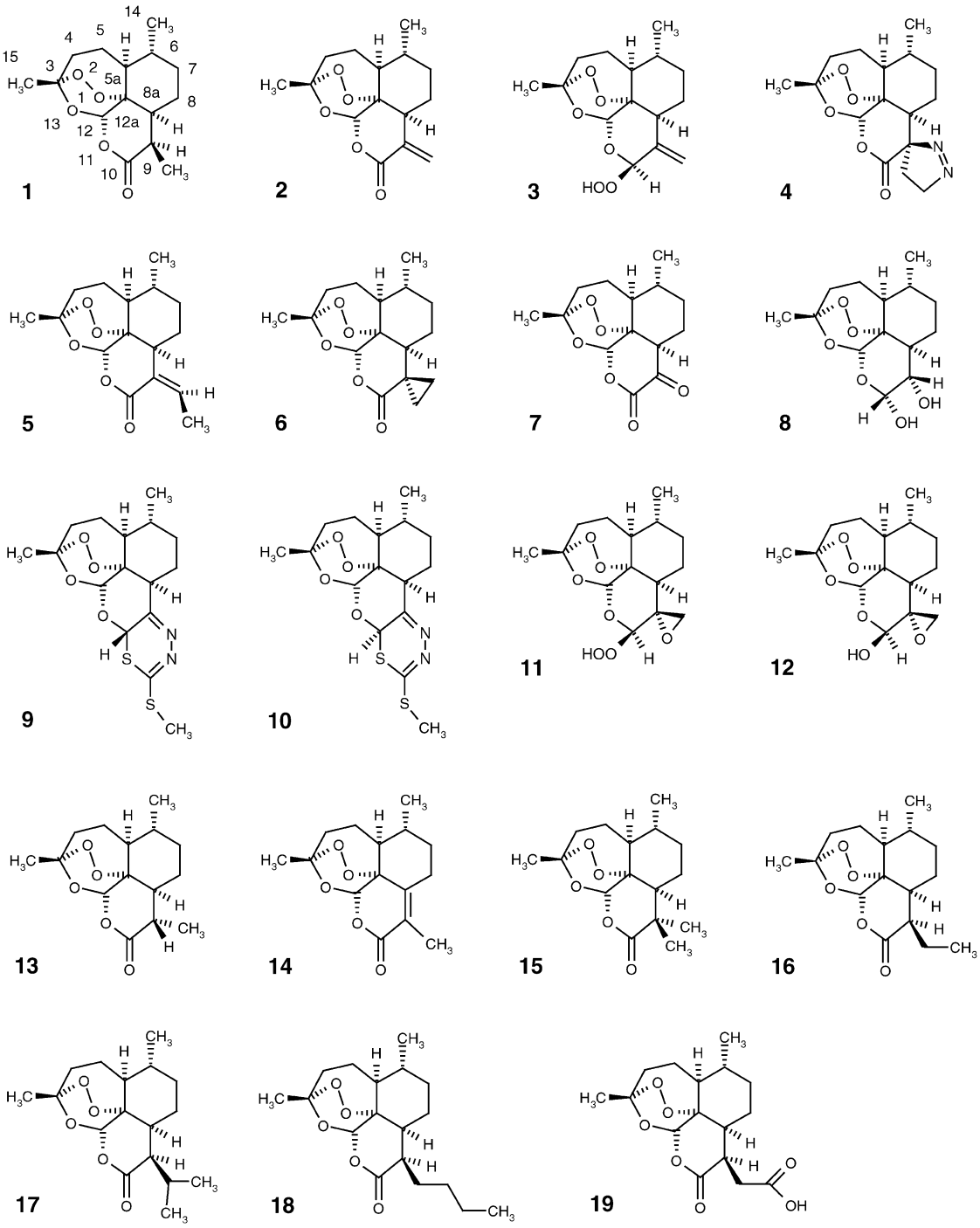

Figure 1. Artemisinin derivatives with antimalarial activity against *Plasmodium falciparum*.

they represent the features necessary to quantify the activity of artemisinin derivatives against ***Plasmodium falciparum***. Therefore, descriptors that show small correlation to the activity (0.7 for all descriptors, 0.6 – 0.7 in some exceptional cases) were discarded. Among those highly correlated, it was selected the ones which can be easier interpreted.

2.2 Chemometrics

Partial Least Squares (PLS) method [41, 42] was employed to construct the PLS model on autoscalled data for 14 artemisinin derivatives, and the model was validated through a leave-one-out cross-validation procedure and

© 2003 WILEY-VCH Verlag GmbH & Co. KGaA, Weinheim

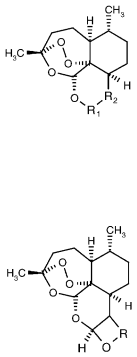

Molecule	R_1	R_2	R
20	C=NH	$C(H)CH_3$	
21	C=S	$C(H)CH_3$	
22	C=O	$C_4H_6O_2$	
23	C=O	$C_9H_8O_2$	
24	C=O	C(H)CHO	
25	C=O	$C_6H_6O_2$	
26			$C_3H_4O_2$
27			$C_9H_{10}O_2$
28			$C_5H_6O_2$
29	C=O	$C(H)C_3H_5O_2$	

Figure 2. New proposed artemisinin derivatives with unknown antimalarial activity against *Plasmodium falciparum.*

calculation of activities for 5 molecules from the external validation set (**6**, **9**, **12**, **17**, **18**). Hierarchical Cluster Analysis HCA and Principal Component Analysis PCA [27] on the same autoscalled data was performed for 19 molecules by using PIROUETTE program [43]. Incremental linkage method was used in HCA.

2.3 Molecular Graphics and Modeling

Database search. The search for the best structures of artemisinin, artemisinin derivatives and heme in the CSD November 2002 release ($R \leq 7\%$), and the structures of oxy- and deoxyhemoglobin and hemoglobin-polyatomic substrate complexes in PDB [34] was performed. As there were only a few hits, the PDB retrieval included later on the best structures of heme-containing proteins (resolution ≤ 1.2 Å).

Molecular graphics. Molecular graphics was performed by using molecular visualization and modeling software PLATON [44], WebLab ViewerLite [45] and Titan [46].

Molecular modeling. Heme, proximal histidine and the oxygen molecule coordinated to the heme iron atom from experimental structure of oxy-myoglobin [47] (PDB: 1A6M, resolution 1.00 Å, $R = 12.2$) were used to build artemisinin-heme-proximal histidine complex. The oxygen molecule served as −O−O− of artemisinin, whose geometry was optimized by using MMFF94 [48] in Titan. Proximal histidine, porphyrin and the propionate directed to the histidine were frozen in all calculations. Methyl and vinyl groups and also the propionate directed to artemisinin, as well as artemisinin, were treated as free in geometry optimizations. This choice of partial freezing of complex geometry showed to be necessary as molecular mechanics as well most of semi-empirical methods do not reproduce well geometry around Fe and of porphyrine system, while *ab initio* calculations could significantly delay. It was supposed that O1 from artemisinin binds Fe from heme covalently, as

Table 1. Experimental and calculated geometrical parameters of the 1,2,4-trioxane ring for artemisinin

	HF/6–31G* (this work)	HF/6–31G*[a]	HF/6–31G[b]	Experimental[c]	Experimental[d]
Bond lengths (Å)					
O1–O2	1.390	1.390	1.447	1.474(4)	1.469(2)
O2–C3	1.396	1.396	1.435	1.418(4)	1.416(3)
C3–O13	1.408	1.408	1.435	1.451(4)	1.445(3)
O13–C12	1.376	1.376	1.403	1.388(4)	1.380(3)
C12–C12a	1.532	1.532	1.533	1.528(5)	1.523(2)
C12a–O1	1.429	–	1.469	1.450(4)	1.462(3)
Bond angles (degree)					
O1O2C3	109.5	109.5	108.8	107.7(2)	108.1(2)
O2–C3–O13	107.8	107.8	106.8	107.1(2)	106.6(2)
C3–O13–C12	115.3	115.3	117.3	113.6(3)	114.2(2)
O13–C12–C12a	112.3	112.3	112.3	114.7(2)	114.5(2)
C12–C12a–O1	110.5	–	110.9	111.1(2)	110.7(2)
C12a–O1–O2	112.7	–	113.2	111.5(2)	111.1(1)
Torsion angles (degree)					
O1–O2–C3–O13	– 73.4	– 73.4	– 71.8	– 75.5(3)	– 75.5(2)
O2–C3–O13–C12	31.1	31.1	33.4	36.3(4)	36.0(2)
C3–O13–C12–C12a	27.4	27.4	25.3	24.7(4)	25.3(2)
O13–C12–C12a–O1	– 50.1	–	– 49.4	– 50.8(4)	– 51.3(2)
C12–C12a–O1–O2	10.9	–	12.5	12.2(3)	12.6(2)
C12a–O1–O2–C3	48.7	–	46.7	47.7(3)	47.8(2)

[a] Values from Ref. 12.
[b] Values from Ref. 18.
[c] Values from Ref. 31. Experimental estimated standard deviations in brackets.
[d] Values from Ref. 32. Experimental estimated standard deviations in brackets.

© 2003 WILEY-VCH Verlag GmbH & Co. KGaA, Weinheim

Table 2. Descriptors selected for PLS analysis, experimental $\log IC_{50}$ values and the correlation matrix

Compound	LUMO + 1(hartree)	Q_9	Q_{11}	RDF030m	NH	[a]log IC_{50}
1	0.2102	– 0.0463	– 0.6063	12	8	0
2	0.2072	– 0.3045	– 0.6484	12	6	0.447
3	0.2137	– 0.2299	– 0.7625	11	6	0.301
4	0.1839	1.0207	– 0.4753	16	6	2.45
5	0.2090	– 0.4382	– 0.7149	13	7	0.0414
6	0.2094	– 0.1482	– 0.6590	13	7	0.716
7	0.1978	0.4336	– 0.5564	13	6	2.23
8	0.2182	0.0517	– 0.5070	14	6	0.580
9	0.1655	0.3708	– 0.4804	24	6	2.48
10	0.1561	0.5379	– 0.2222	22	6	2.48
11	0.2165	– 0.3053	– 0.7893	13	7	– 0.0458
12	0.2181	– 0.2834	– 0.8116	13	7	– 0.0458
13	0.2071	0.1139	– 0.5893	13	7	0.261
14	0.2053	– 0.1689	– 0.5448	9	6	0.631
15	0.2120	0.1487	– 0.5499	16	8	0.518
16	0.2050	– 0.0503	– 0.6532	9	8	– 0.246
17	0.2109	– 0.0152	– 0.5941	15	9	– 0.0938
18	0.2082	– 0.0677	– 0.5983	12	7	– 0.00540
19	0.1852	0.0430	– 0.5857	14	6	0.824
LUMO + 1		– 0.687	– 0.769	– 0.768	0.435	– 0.832
Q_9			0.744	0.577	– 0.273	0.832
Q_{11}				0.638	– 0.275	0.722
RDF030 m					– 0.202	0.706
NH						– 0.604

[a] IC_{50} nmol/mL relative to IC_{50} for artemisinin in Figure 1 (compound **1**).

some recent docking studies have demonstrated recently [49]. Complexes including derivatives **8**, **29**, **31** were built by modification of artemisinin from the MMFF94 optimized complex. Two active (**1**, **26**) and two non-active (**7**, **24**) artemisinins were selected to perform the MMFF94 conformational search about Fe–O1 systematically, by fixing torsion angle O2–O1–Fe–C (C from porphyrin, *meso* position between the two propionate groups) to 0°, ±15°, ±30°, ..., ±165°, 180° (negative angle is in clockwise direction from the *meso*-C). Plots of MMFF94 energy *vs.* O2–O1–Fe–C angle (not represented) showed the same form for all complexes, and that the global minima were concentrated in region −105° to −135°. Structures of the complexes with angle −120° were considered as the most stable. The final MMFF94 optimization of the complexes was performed by using the unconstrained angle of the most stable conformers.

Docking of some artemisinins to hemoglobin. Docking of **1**, **7**, **24**, **26** and **29** to heme, based on the preferential orientation for the ligands observed in the MMFF94 conformational studies, was performed by Titan. Artemisinin from the artemisinin-heme-proximal histidine complex was incorporated into the A chain of hemoglobin A after replacing the original ligand by artemisin (PDB: 2HBE [50]). Derivatives **7**, **24**, **26** and **29** were obtained by modifying the docked artemisinin.

3 Results and Discussion

PCA and HCA analysis. Five molecular descriptors were selected for data analysis. The descriptors (LUMO + 1, Q_9, Q_{11}, NH and RDF030 m), the experimental values of activity IC_{50} for the antimalarial artemisinin derivatives, and correlations including all data for 19 molecules can be seen in Table 2. The correlation between descriptors is less than 0.77, as can be seen in Table 2. The first three Principal Components PCs describe 91.79% of the original information for the first 19 molecules. The PC1-PC2 scores and loadings plot are shown in Figures 3 and 4. From Figure 3, one can see that the molecules are distributed into three distinct regions mainly in PC1. The highly active compounds are on the left side (**1**, **5**, **11**, **12**, **16 – 18**) and the less active are on the right side (**4**, **9**, **10**,).

Hierarchical cluster analysis (HCA) [27], gives results, which are similar to those in PCA (see dendogram in Figure 5). The compounds are fairly grouped according to their activity. The minus cluster contains less active compounds with π-bond rings at C9 and C10 (**4**, **9**, **10**). There are two clusters of moderately active compounds, the small one with C=O groups incorporated in the substituent at C9 (**7**, **19**), and the big one with different small substituents at C9 and/or C10 (**2**, **3**, **6**, **8**, **13**, **14**, **19**). Molecule **18**, although among highly active in PCA, is positioned with moderately active compounds probably due to its long chain at C9. Two clusters of highly active compounds include predominantly

© 2003 WILEY-VCH Verlag GmbH & Co. KGaA, Weinheim

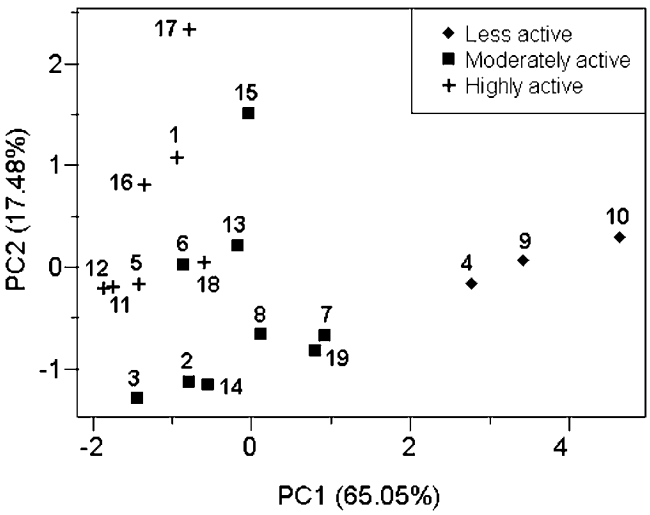

Figure 3. PC1-PC2 scores plot for the 19 artemisinin derivatives with antimalarial activity against *Plasmodium falciparum.*

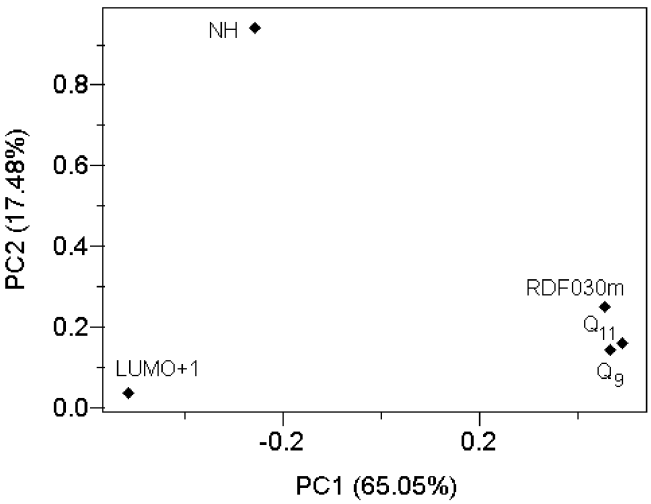

Figure 4. PC1-PC2 loadings plot using the five descriptors selected to build the PLS model for the 19 artemisinin derivatives with antimalarial activity against *Plasmodium falciparum.*

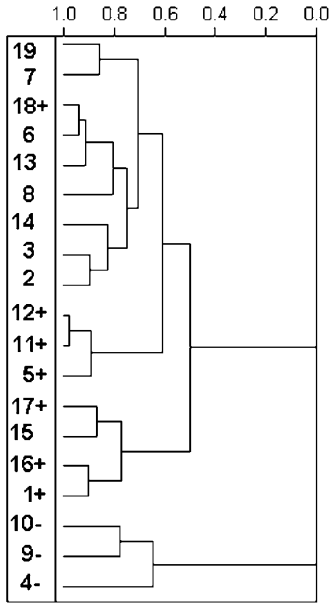

Figure 5. HCA dendogram for 19 artemisinins with highly active (plus sign), moderately (no sign) and less active (minus sign) compounds.

alkyl substituents at C9 (**1**, **5**, **11**, **12**, **16**, **17**, **18**) and moderately active **15** with alkyl substituents at the same position. **11** and **12** have similarity index 0.98, what agrees with their structural similarity and identical activity.

According to Figure 4 the highly active compounds have main contribution of LUMO + 1 and NH, while the less active have major contribution of Q_9, Q_{11} and RDF030m descriptors. The negative correlation of LUMO + 1 with the log IC_{50} indicates that radical reactions, as heme-mediated artemisinin activation by cycloalkane ring openings [4], might be in question. Some high energy interaction (Fe–O bonding, hydrogen bond or polar interaction) or many weak interactions (hydrophobic) may be related also to NH and LUMO + 1. As many artemisinin derivatives have electronegative atoms in C9 and/or C10 substituents, mostly oxygen atoms, such interactions might be expected. Partial atomic charges at C9 (Q_9) and O11 (Q_{11}) are positively correlated to log IC_{50}. High valence electronic density in C9 substituents (mainly electronegative atoms involved in double bonds) means that Q_9 becomes more positive (**4**, **7**–**10**). In some cases this can lower the activity, specially when decreasing NH. On the other hand, conformational properties around C9 are mostly unfavorable for artemisinin ring to approach heme (**4**, **7**, **9**, **10**). Less negative Q_{10} means having small charge in the neighboring C10, and so the artemisinin polar area is reduced. This is very much pronounced for compounds **4**, **7**, **9**, **10** where electron delocalization/conjugation weakens the artemisinin polar area, and also changes the ring conformation to be more planar moving the ring farther from the porphyrine plane.

NH is a variable which describes the C–H ... π interactions of artemisinin with heme. Hydrogen atom in a C–H bond which is nearly perpendicular to the heme plane, and at distance up to 3.1 Å from the plane satisfies the geometrical conditions for C–H ... π interactions which are important in organic synthesis, crystal packing and biological events (activity), especially in heme – amino-acid interactions in hemoglobin [49]. In artemisinin, two hydrogen atoms at C9 are available for more than one C–H ... π interaction. These interactions weaken or disappear due to substitution by large cyclic groups (**4**, **9**, **10**), hydrogen deficient groups (**2**, **3**, **7**), or by other modifications (**8**, **13**, **14**).

PLS modeling. QSAR model was built by PLS using 14 compounds (calibration set). Three PCs showed to be significant and explained 89.55% of the total variance. In

 © 2003 WILEY-VCH Verlag GmbH & Co. KGaA, Weinheim

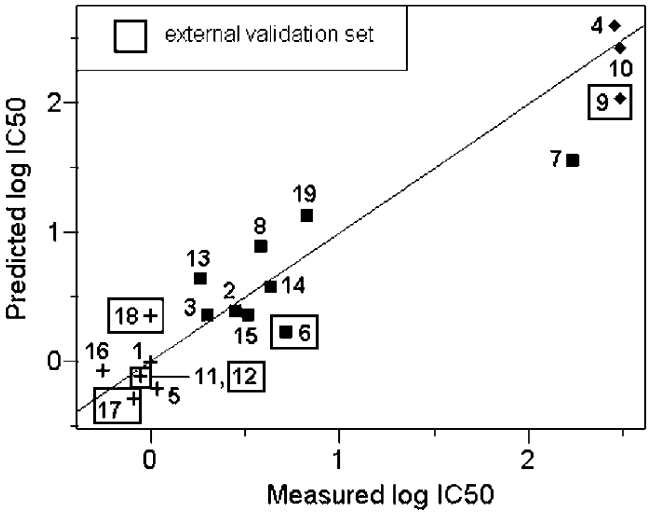

Figure 6. Measured versus the predicted log IC_{50} by PLS model using three PCs. Symbols have the same meaning as in Figure 4.

Figure 6 is shown the plot of the correlation between the measured and the predicted log IC_{50} for the 3 PCs model, where the highly active compounds are located in its lower part. Samples from the external validation set (**6**, **9**, **12**, **17**, **18**) are included also. Molecule **7** was classified as moderately active by PCA and HCA, but is less active according to experimental and predicted activities (Table 2). The quality of the PLS model can be better demonstrated by the SEP, Q^2 and R^2 parameters and by numerical comparison between the measured and predicted activities, all listed in Table 3. From this table, one can see that the statistical parameters are quite meaningful ($Q^2 = 0.83$, $R^2 = 0.92$) and the agreement between measured and predicted values is in general quite satisfactory, taking into account that artemisinin is a complicated molecular system. Predicted IC_{50} values for the external validation set (Table 3) agree well with experimental data for **12** and **17**, while **6** and **9** are overpredicted and **18** underpredicted by less than 0.5 in IC_{50} units. The regression model was applied to predict the unknown antimalarial activity of ten new artemisinin derivatives included in Figure 2 (prediction set, Table 4). Artemisinin derivative **26** is predicted to be more active than any among **1**–**19** with known antimalarial activity, while **20**, **28** and **29** have activities predicted higher than artemisinin and even some other highly active compounds (**5**, **11**, **12** and **16**). Thus, compounds **20**, **26**, **28** and **29** can be considered as new potent antimalarial artemisinins.

Classical molecular descriptors had lower correlation with activity than selected descriptors and/or produced worse PLS models: molecular weight (0.598), HOMO (0.553), LUMO (−0.664), molecular refractivity (0.538), logP (−0.620). Pictorial representation of frontier orbitals clearly shows that there is practically no distinction in the activity classes based on HOMO or LUMO orbitals (results not shown). The distinction can be clearly noticed when

Table 3. Experimental and estimated antimalarial activity (log-IC_{50}) by PLS[a] and the goodness of the model.

Compound	Experimental	Estimated	Residuals
1	0	−0.0198	0.0198
2	0.447	0.383	0.064
3	0.301	0.352	−0.051
4	2.45	2.59	−0.14
5	0.0414	−0.205	0.247
6*	0.716	0.220	0.496
7	2.23	1.55	0.68
8	0.580	0.893	−0.313
9*	2.48	2.03	0.45
10	2.48	2.42	0.06
11	−0.0458	−0.123	0.0772
12*	−0.0458	−0.118	0.0717
13	0.261	0.637	−0.376
14	0.631	0.572	0.059
15	0.518	0.350	0.168
16	−0.246	−0.0691	−0.177
17*	−0.0938	−0.288	0.194
18*	0.00540	0.349	−0.344
19	0.824	1.13	−0.307

Descriptors	LUMO + 1	Q_9	Q_{11}	RDF030m	NH
Regr. vector	−0.156	0.577	0.073	0.077	−0.339

Q^2	SEP	R^2
0.833	0.375	0.917

[a] PLS models using three principal components and leave-one-out cross-valiation.
* Samples from the external validation set.

Table 4. Predicted antimalarial activity (logIC_{50}) for the compounds in Figure 2

Compound	[a]log IC_{50}
20	−0.0250
21	0.103
22	0.752
23	0.801
24	0.437
25	0.749
26	−0.382
27	0.234
28	−0.228
29	−0.0400

[a] IC_{50} nmol/mL relative to IC_{50} for artemisinin in Figure 1 (compound **1**).

LUMO + 1 orbitals are compared, as is shown in Figure 7 where one can see a representative molecule with high (**1**) and low (**9**) activity from the training & external validation set, and also a derivative with high (**26**) and low (**23**) predicted activities. LUMO + 1 orbital lobes in highly active compounds are positioned mainly on atoms C4–C8a, C14 and corresponding hydrogen atoms. Some lobes in all such compounds are directed towards possible heme position, indicating the importance of C–H...π [51] and other orbital

© 2003 WILEY-VCH Verlag GmbH & Co. KGaA, Weinheim

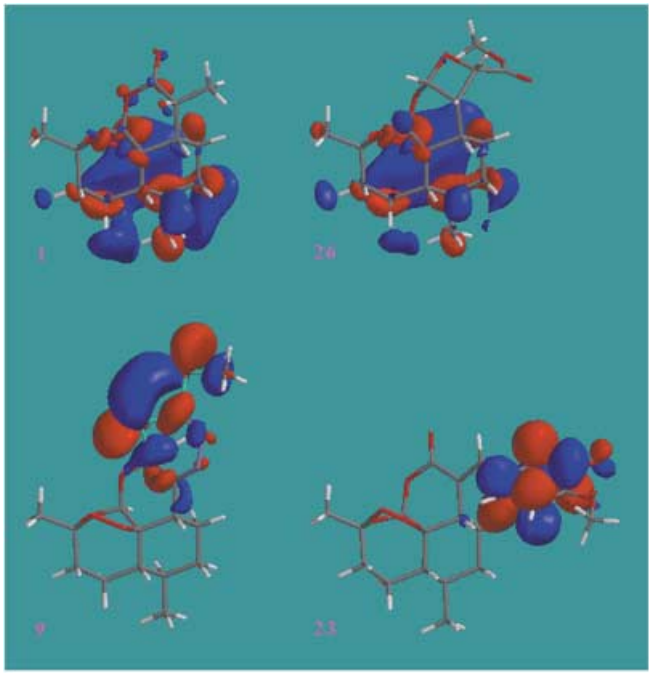

Figure 7. LUMO + 1 orbital for two highly active (**1**, **26**) and less active (**9**, **23**) artemisinins viewing the side that contains peroxide group and can be complexed with heme. Positive lobs are colored blue, and negative are red.

interactions with heme delocalized system. Small lobes on peroxide group can be observed also, while there are very little or no lobes at C9, C10 and substituents at these positions. Less active molecules exhibit LUMO + 1 orbital lobes concentrated mainly on C9, C10 and substituents at these positions. Such substituents are mainly rigid and large and possess π-bonds which do not fit well to heme in spatial sense, and at the same time these substituents overtake the function of orbital overlap with heme what does not provide optimal orbital overlap as in complexes including highly active artemisinins. These factors may explain why molecules with such LUMO + 1 orbital distribution are less active, and why LUMO + 1 energy is a good molecular descriptor in PLS model in this work. Before mentioned radical mechanism of the cycloheptane ring is another possibility to account for large LUMO + 1 lobes at the artemisinin skeleton on its side which does not react with heme.

Artemisinin-heme binding mode. Some O...O non-bonding distances in artemisinin crystal structure are rather short [2.171(3) – 3.073(3) Å in QNGHSU03 [32] and 2.180(4) – 3.072(4) Å in QNGHSO10 [31]], while maximal are around 4.5 Å [4.460(3) Å in QNGHSU03 and 4.443(4) Å in QNGHSU10]. On the other side, there is C–O bond length alteration in artemisinin. The range 1.390(11) – 1.477(8) Å and mean 1.434 Å for C_{sp3}–O(2) bonds in organic crystals was observed by Allen *et al.* [52]. The two artemisinin crystal structures and of artemisinin derivatives from the CSD database, FAWBEK [53], JEXGUO [54], SIKLAZ [55], WIMMEK [56], ZILMUC [57] and ZILNAD [57] ($R < 0.07$, exp. errors for bond lengths < 0.01 Å) exhibit very short (1.34 – 1.36 Å) C10–O11 bond in the presence of double C10=O10, and shortened (1.39 – 1.41 Å) C12–O13 bond. O2–C3, C12–O13, C10–O11 bonds are significantly shortened, O1–O1a, C3–O13, O11–C12 lengthened with respect the standard mean 1.434 Å. Probably steric (the presence of quaternary carbon) and electronic (conjugation, hyperconjugation) effects are responsible for the bond length alteration. Jiang *et al.* [58] noticed that C–O bond orders and other electronic properties for peroxide group and O10 can be QSAR descriptors. It is highly possible that the oxygens are connected to each other *via* mechanism of through-bond and through-space interactions [59]. Thus, substituent and conformation effects might affect the charge distribution at the oxygens, and even Fe–O bond. Recent experimental evidences for O...π through-space interactions [60, 61] indicate that some artemisinin oxygens, that from the peroxyde group which is not bound to iron, could participate in such interactions. A recent finding by Ziegler *et al.* [62] "that substrate recognition is based on porphyrin moiety rather than specific metal recognition", supports the possibility of various heme-artemisinine non-bonding interactions.

MMFF94 conformational search around Fe–O bond for the four heme-ligand complexes (ligands – **1**, **7**, **24**, **26**) revealed practically the same Fe coordination geometry. Significant differences are observed in ligand conformation and its orientation with respect to the heme, and in conformation of the free propionate chain. Descriptor NH used in PLS can be visualized through the number of artemisinin hydrogens which are placed at most 3.1 Å from the heme carbons and the number of C–H...π interactions involving these hydrogens: active compounds **1** and **26** have 6 hydrogens included in 19 (**1**) or 18 (**26**) C–H...π interactions, less active **7** has 4 hydrogens in 6 such interactions, and **24** has 6 hydrogens participating in 20 C–H...π interactions. C10=O10 bond in **1**, **7**, **24** is close to the *meso*-CH between the propionates (at distance being 2.9 – 3.1 Å). C9=O in **24** is parallel to the closest pyrrole at short distance (≈ 3.2 Å). These C=O...π through-space interactions could additionally stabilize the complexes. The free (not frozen in calculations) propionate is directed towards C9, C10 substituents in **1**, **24**, **26** *via* polar-polar interactions, but is apart from them in **7** (Figure 8). Although the geometry of the complexes explains most of molecular descriptors in PLS/HCA study, the heme-ligand mode stays partially unexplained in terms of ligand-protein orientation.

Search for experimental heme-containing crystal structures with high accuracy and low resolution in CSD and PDB databases confirmed the findings from MMFF94 conformational study. There are a few heme-ligand complexes, where ligand is a polyatomic molecule inside hemoglobines (nicotinate in 1FSL [63], Figure 9 left; *N*-butyl isocyanide in 2HBE [50]; *N*-propyl isocyanide in

© 2003 WILEY-VCH Verlag GmbH & Co. KGaA, Weinheim

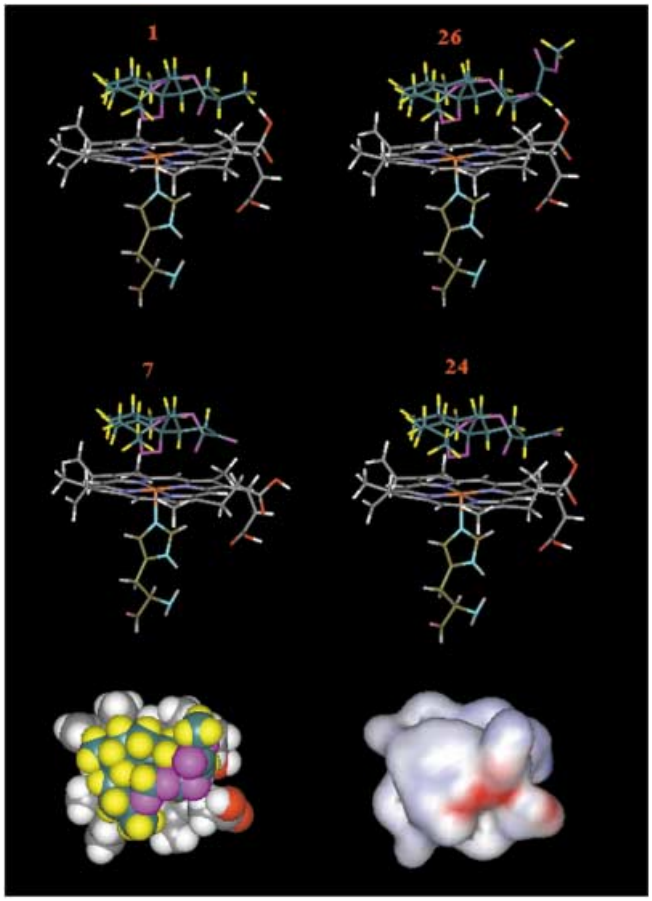

Figure 8. A proposed heme-ligand binding mode based on MMFF94 calculations with the four ligand (**1**, **8**, **24**, **26**) preferencial orientation. Top view of complex with **1** is shown below in space-filling and electrostatic potential representation.

2HBF [50]) or in free heme-ligand complex (*p*-nitrotiolate in NTPROT10 [64]). The most accurate cytochrome structure (1CTJ [65]) includes *N*-butyl isocyanide as the heme ligand. Orientation of the ligand with respect to heme exhibits well defined regularities already observed in the MMFF94 conformational study: polar/hydrophobic parts of the ligand are directed towards the polar (Fe-N central area and the propionates)/hydrophobic (methyl and vinyl groups opposite to the propionate groups) parts of the heme system (see Figure 9 left).

It is known that the main amino-acid residues that occlude the space above the heme in hemoglobin are mostly hydrophobic (Lys E10, Val E11, Leu G8, Phe CD4, His E7) [66]. More general map of polar/hydrophobic group distribution (including ligands, residues, solvents) around heme was constructed (Figure 9 right) based on heme-ligand structures, where ligands are proximal histidine and polyatomic molecules (PDB: 1FSL, 2HBE, 2HBF) in human or soya bean hemoglobine, and diatomic or polyatomic molecules (CSD: NTPTOT10, $R = 7.1\%$, methoxy derivative of heme; PDB: 1A6M, 1C75 [67], 1CTJ, $R < 14\%$, resolution < 1.1 Å) in various heme-containing proteins (except NTPROT10, where heme is alone) from the most accurate crystal structures. The placement of two polyatomic molecules nicotinate (9 non-H atoms; PDB: 1FSL, Figure 9 left) and *N*-butyl isocyanide (8 atoms; PDB: 2HBE) can be useful as a model for artemisinin (20 atoms) binding. The presented crystal structures exhibit well that amino-acids are oriented to the heme and the ligands so that more polar/hydrophobic amino-acids or their fragments are directed towards proximal polar/hydrophobic parts of heme-ligand complex. Artemisinin molecule in crystal structure (CSD: QNGHSU03) participates in 40 interac-

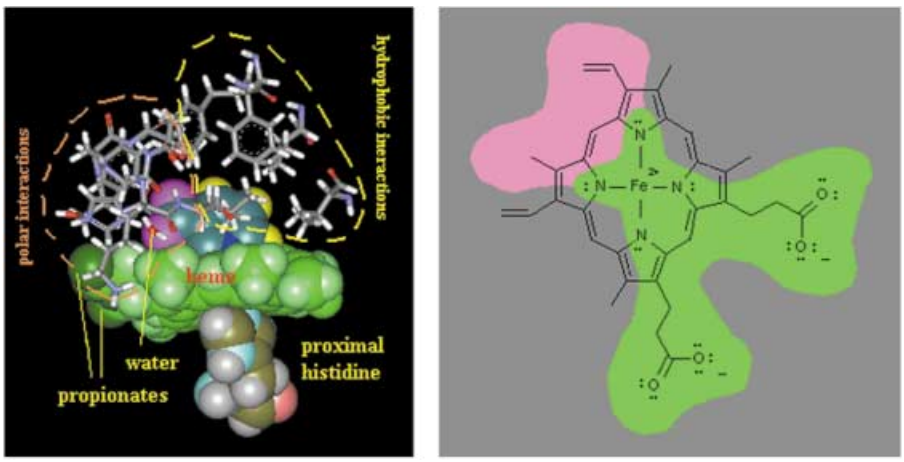

Figure 9. Left: An example of retrieved heme-containing crystal structures from the PDB database: Heme (green) complexed with nicotinate (PDB: 1FSL [63]) and proximal histidine. The closest amino-acid residues and a water molecule are presented also. Right: The average hydrophobic character of ligands and residues around heme based on retrieved crystal structures from the CSD and PDB databases: predominantly polar (green), hydrophobic (pink) and amphiphilic (gray).

© 2003 WILEY-VCH Verlag GmbH & Co. KGaA, Weinheim

tions: weak hydrogen bonds C–H...O, and weak contacts C–H...H–C. Shukla *et al.* [68] reported that the main contribution to binding to heme have hydrophobic interactions, but the specificity of the binding is contributed by hydrogen bonds and electrostatic interactions (this can be noticed for nicotinate in Figure 9 left). Substituent side chains on artemisinin could interact even more with the surrounding flexible residues (it is known that positional displacement of the residues goes up to 6 Å during oxygenation [66]), but the main binding contribution remains to heme-artemisinin interaction. Orientation of artemisinin derivatives with respect to polar-polar and hydrophobic-hydrophobic interactions is reasonable. Grigorov *et al.* [5] concluded that the antimalarial activity of certain 1,2,4-trioxanes requires two hydrophobic sites located at heme and a hydrogen bond donor site, probably from solvent (as is the case in hemoglobin – nicotinate complex, see Figure 9 left). Furthermore, they noticed that face-to-face π...π stacking between phenyl and pyrrole contribute to binding.

A recent artemisinin – heme docking study [49] rationalized the artemisinin antimalarial activity: 1) the biological activity is highly correlated to heme-drug binding energy, and moderately to weakly to Fe–O distances (excluding O10); 2) long hydrophobic chain substituents at C9 (equatorial positions) weakens the binding to heme, even in the absence of O10; 3) hydrophobic substituents at C3 (equatorial) can also involve in interactions with the porphyrine system; 4) C10 substituents, if having both polar and aromatic groups, can increase the activity. Docking study in this work included heme-ligand (ligand = **1**, **7**, **24**, **26**) interactions in monomer unit of hemoglobin A. In general, the docking results are in accordance with MMFF94 conformational search and the CSD/PDB database structural observations on ligand-heme stereoelectronic relationships.

Figure 10 represents heme-proximal histidine-**26** complex. The main differences in the four ligand-hemoglobin complexes are in region including C9, C10 substituents. The placement of polar/hydrophobic amino-acids and their fragments follow the distribution map in Figure 9 right. 3-Me and 6-Me are positioned into small hydrophobic pockets. Big amphiphilic pocket formed by proximal His 58, Gly 59, Lys 61, Val 62, Ala 63, Leu 83, Asp 64 can bury the heme propionates with neighboring Me, and C9, C10 substituents. Introducing O atoms into C9 substituent (**26**), the artemisinin polar area increases and also the space with polar interactions between heme, ligand and globin; as a consequence, terminal Me group of the C9 substituent in **26** penetrates the pocket up to the hemoglobin surface, close to the channel formed by insertion of heme into globin (see Figure 11). This placement of C9 substituent with respect to the globin can explain the highly predicted antimalarial activity of **26**. MMFF94 conformational study revealed that –C9(H) –CH_x fragment (x = 1, 2, 3) in artemisinins is placed between the CH_2 of the closer propionate and the closest Me

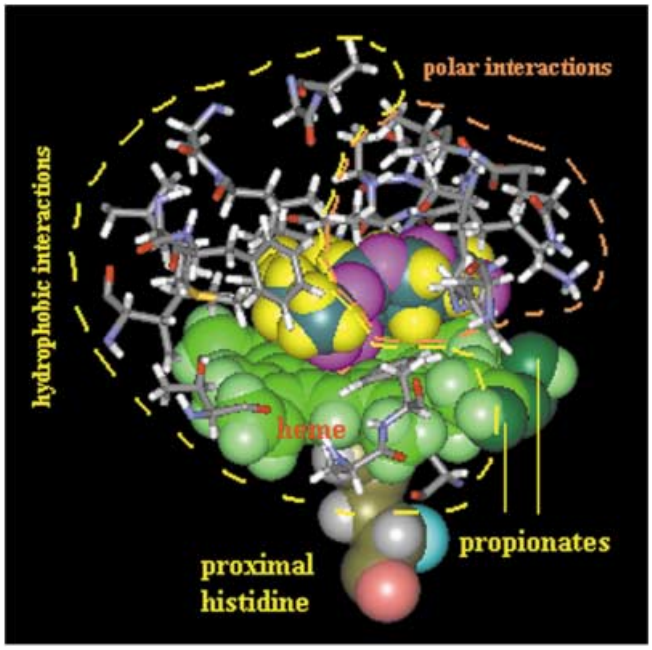

Figure 10. Artemisinin derivative **26** docked to hemoglobin A (A chain from 2HBE [50]) and optimized by MMFF94, shown surrounded by some twenty closest amino-acids.

in the heme molecule. The docking study shows that this hydrophobic fragment is situated in a small hydrophobic sub-pocket, which is completed with hydrophobic parts of Lys 61, Val 62 and Gly 59 residues. C10=O10 group in **7** is involved in unexpected hydrogen bond with N–H of the proximal histidine. Besides, C9=O group falls into the small hydrophobic sub-pocket, what results in unfavorable polar-hydrophobic interaction. The intermolecular forces can turn **7** from the best position required for artemisinin activation. **24** possesses polar substituent at C9 participating polar-hydrophobic interactions. This can be a reason for **24** being less active, but still more active than **7**. **29** shows similar behavior as **26**. Figure 11 exhibits different stage of C9,C10 ligand extension to the protein exterior in terms of its projected surface area (green) which is proportional to antimalarial activity (results not shown).

4 Conclusions

Significant regression model was obtained by PLS method for artemisinin derivatives with antimalarial activity against *Plasmodium falciparum* reported in literature, based on the descriptors LUMO + 1 energy, charges Q_9 (C9) and Q_{11} (O11), number of hydrogen atoms NH and a radial distribution function RDF030 m. The regression model showed statistical significance but also predictive ability and revealed that higher values for the LUMO + 1 combined with high negative charges on the atoms C9 (Q_9) and O11

© 2003 WILEY-VCH Verlag GmbH & Co. KGaA, Weinheim

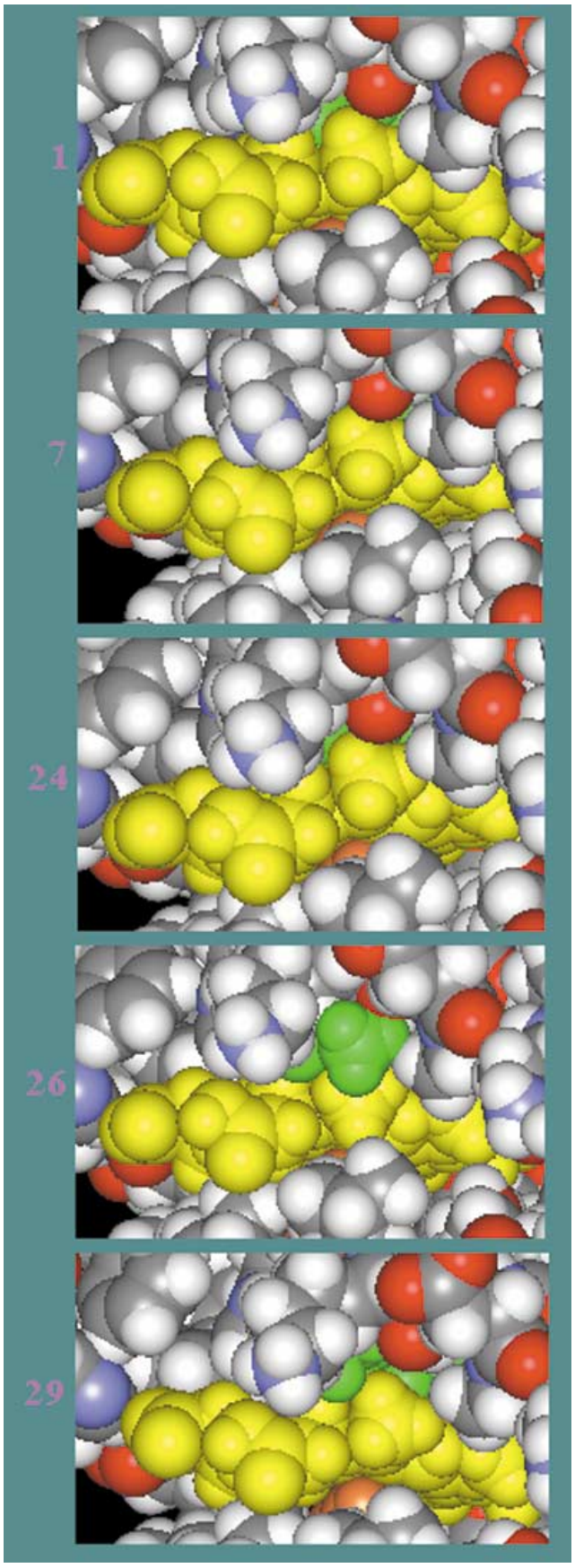

◀ **Figure 11.** Space-filling model of complexes hemoglobin-ligand (ligand: **1**, **7**, **24**, **26**, **29**), in region around C9, C10 substituent, showing heme (yellow), proximal histidine (orange), and the artemisinin derivative (green).

(Q_{11}), higher NH and lower values for RDF030m increase the antimalarial activity against *Plasmodium falciparum*.

A new artemisinin derivative **26** was predicted to be active against *Plasmodium falciparum* resistant to mefloquine higher than the compounds reported in literature. Synthesis of novel artemisinin derivatives as potent antimalarial drugs may follow the results of quantum chemical and Partial Least Squares methods in this work, supported by molecular graphics, modeling and structural studies. Compounds **26** and **29** are the most active in the prediction set, and both possess equatorial C9 substituents with polar and hydrophobic groups which are able to fit into corresponding polar/hydrophobic regions of the hemoglobin pockets, and even to extend to the hemoglobin exterior.

Acknowledgements

The authors thank to IQ-Araraquara for using GaussView program, to Brazilian agencies CNPq and FAPESP for finantial support, and to CENAPAD-UNICAMP for computational support.

References

[1] A. R. Butler, Y.-L. Wu, The nonenzymatic cyclic dimerization of 5-aminolevulinic acid, *Chem Soc. Rev.* **1992**, *21*, 85 – 90.
[2] S. Bowman, D. Lawson, D. Basham, D. Brown, T. Chillingworth, C. M. Churcher, A. Craig, R. M. Davies, K. Devlin, T. Feltwell, S. Gentles, R. Gwilliam, N. Hamlin, D. Harris, S. Holroyd, T. Hornsby, P. Horrocks, K. Jagels, B. Jassal, S. J. Kyes, S. McLean, S. Moule, K. Mungall, L. Murphy, R. K. Olive, M. A. Quail, M.-A. Rajadream, S. Rutter, J. Skelton, R. Squares, S. Squares, J. E. Sulston, S. Whitehead, J. R. Woodward, C. Newbold, B. G. Barrell, The complete nucleotide sequence of chromosome 3 of Plasmodium falciparum, *Nature* **1999**, *400*, 532 – 538.
[3] A. V. Pandey, B. L. Tekwani, R. L. Singh, V. S. Chaudan, Artemisinin, an Endoperoxide Antimalarial, Disrupts the Hemoglobin Catabolism and Heme Detoxification System in Malarial Parasite, *J. Biol. Chem.* **1999**, *274*, 19383 – 19388.
[4] S. Kamchonwongpaisan, E. Samoff, S. R. Meschinck, Identification of Hemoglobin Degradation Products in Plasmodium Falciparum, *Mol. Biochem. Parasitol.* **1997**, *86*, 179 – 186.
[5] M. Grigorov, J. Weber, J. M. J. Tronchet, C. Jefford, W. K. Milhous, D. Maric, A QSAR study of the antimalarial activity of some synthetic 1,2,4-trioxanes, *J. Chem. Inf. Comput. Sci.* **1977**, *37*, 124 – 130.
[6] M. A. Avery, F. Gao, W. K. M. Chong, S. Methrotra, W. K. Millhous, Structure-activity-relationships of the antimalarial agent artemisinin. 1. Synthesis and comparative molecular-

© 2003 WILEY-VCH Verlag GmbH & Co. KGaA, Weinheim

field analysis of C-9 analogs of artemisinin and 10-deoxoartemisinin, *J. Med. Chem.* **1993**, *36,* 4264 – 4275.
[7] M. A. Avery, S. Mehrotra, T. L. Johnson, J. D. Brak, J. A. Vroman, R. Miller, Structure-activity relationships of the antimalarial agent artemisinin. 5. Analogs of 10-deoxoartemisinin substituted at C-3 and C-9, *J. Med. Chem.* **1996**, *39*, 4149 – 4155.
[8] P. M. O'Neill, D. J. Willock, S. R. Hawley, P. G. Bray, R. C. Storr, S. A. Ward, B. K. Park, Synthesis, antimalarial activity, and molecular modeling of tebuquine analogues, *J. Med. Chem.* **1997**, *40*, 437 – 348.
[9] D. Y. D. De, F. M. Krogstad, L. D. Byers, Structure-activity relationships for antiplasmodial activity among 7-substituted 4-aminoquinolines, *J. Med. Chem*, **1998**, *41*, 4918 – 4926.
[10] P. M. O'Neill, N. L. Searle, K.-W. Kan, R. C. Storr, J. L. Maggs, S. A. Ward, K. Raynes, B. K. Park, Novel, potent, semisynthetic antimalarial carba analogues of the first-generation 1,2,4-trioxane artemether, *J. Med. Chem.* **1999**, *42*, 5487 – 5493.
[11] H. U. Suter, D. M. Maric, J. Weber, C. Thomson, Quantum chemistry and drug design, *Chimia* **1995**, *49*, 125 – 127.
[12] G. Bernardinelli, C. W. Jefford, D. Maric, C. Thomson, J. Weber, Computational studies of the structures and properties of potential antimalarial compounds based on the 1,2,4-trioxane ring structure. 1. Artemisinin-like molecules, *Int. J. Quant. Chem.: Quant. Biol. Symp. Suppl.* **1994,** *21*, 117 – 131.
[13] A. K. Bhattacharjee, J. M. Karle, Molecular electronic properties of a series of 4-quinolinecarbinolamines define antimalarial activity profile, *J. Med. Chem.* **1996**, *39*, 4622 – 4629.
[14] S. Kokpol, S. V. Hannongbua, N. Thongrit, S. Polman, B. M. Rode, M. G. Schwendinger, Analysis of structure activity relation for primaquine antimalarial-drugs by a quantum pharmacological approach, *Anal. Sci.* **1988**, *4*, 565 – 568.
[15] S. Polman, S. Kokpol, S. V. Hannongbua, B. M. Rode, Quantum pharmacological analysis of structure activity relationships for mefloquine antimalarial-drugs, *Anal. Sci.* **1989**, *5*, 641 – 644.
[16] B. M. Rode, M. G. Schwendinger, S. Kokpol, S. V. Hannongbua, S. Polman, Quantum pharmacological studies on antimalarial-drugs, *Monatsh. Chem.* **1989**, *120*, 913 – 921.
[17] V. Nguyen-Chong, B. M. Rode, Quantum pharmacological analysis of structure-activity relationships for mefloquine antimalarial drugs using optimal transformations, *J. Chem. Inf. Comput. Sci.* **1996**, *36*, 114 – 117.
[18] J. C. Pinheiro, M. M. C. Ferreira, O. A. S. Romero, Antimalarial activity of dihydroartemisinin derivatives against *P. falciparum*: a quantum chemical and multivariate study, *J. Mol. Struct. (Theochem)* **2001**, *572*, 35 – 44.
[19] D. L. Klayman, Qinghaosu (Artemisinin): an antimalarial drug from China, *Science* **1985**, *228*, 1049 – 1055.
[20] Y. L. Hon, Y. Z. Yang, S. R. Meschnick, The Interaction of Artemisinin with Malarial Hemozoin, *Mol. Biochem. Parasitol.* **1994**, *63*, 121 – 128.
[21] D. Y. Wang, Y. L. Wu, A possible antimalarial action mode of qinghaosu (artemisinin) series compounds. Alkylation of reduced glutathione by C-centered primary radicals produced from antimalarial compound qinghaosu and 12-(2,4-dimethoxyphenyl)-12-deoxoqinghaosu, *Chem. Commun.* **2000**, 2193 – 2194.
[22] K. Roy, D. K. Pal, A. Saha, C. Sengupta, QSAR with electrotopological state atom index: Part II – Antimalarial activity of dihydroqinghaosu derivatives, *Indian J. Chem.* **2001**, *B40*, 587 – 595.
[23] N. Acton, J. M. Karle, R. E. Miller, Synthesis and antimalarial activity of some 9-substituted artemisinin derivatives, *J. Med. Chem.* **1993**, *36*, 2552 – 2557.
[24] N. Acton, D. L. Klayman, Conversion of artemisinin (qinghaosu) to iso-artemisitene and to 9-epi-artemisinin, *Planta Med.* **1987**, *53*, 266 – 268.
[25] C. C. J. Roothaan, New Development in Molecular Orbital Theory, *Rev. Mod. Phys.* **1951**, *23*, 69 – 89.
[26] J. W. Hehre, R. Ditchfield, J. A. Pople, Self-consistent molecular-orbital methods. 12. Further extensions of gaussian-type basis sets for use in molecular-orbital studies of organic-molecules, *J. Chem Phys.* **1972**, *56*, 2257 – 2261.
[27] K. R. Beebe, R. J. Pell, M. B. Seasholtz, *Chemometrics: A Pratical Guide*, Wiley, New York, **1998.**
[28] M. M. C. Ferreira, Multivariate QSAR, *J. Braz. Chem. Soc.* **2002,** *13*, 742 – 753.
[29] M. A. Avery, F. Gao, W. K. M. Chong, S. Mehrotra, W. K. Milhous, Structure-Activity Relationships of the Antimalarial Agent Artemisinin. 1. Synthesis and Comparative Molecular Field Analysis of C-9 Analogs of Artemisinin and 10-Deoxoartemisinin, *J. Med. Chem.* **1993,** *36*, 4264 – 4275.
[30] GaussView 1.0, Gaussian, Inc.: Pittsburgh, PA, 1997.
[31] I. Leban, L. Golič, M. Japelj, Crystal and molecular structure of Qinghaosu: a redetermination, *Acta Pharm. Jugosl.* **1988**, *38*, 71 – 77.
[32] J. N. Lisgarten, B. S. Potter, C. Bantuzeko, R. A. Palmer, Structure, absolute configuration, and conformation of the antimalarial compound: Artemisinin,. *J. Chem. Cryst.* **1998**, *28*, 539 – 543.
[33] F. H. Allen, The Cambridge Structural Database: a quarter of a million crystal structures and rising, Acta Cryst. **2002**, *B58*, 380 – 388.
[34] Protein Data Bank, The Rutgers State University, Piscataway, NJ. http://www.rcsb.org/pdb/
[35] M. J. Frisch, G. W. Trucks, H. B. Schlegel, G. E. Scuseria, M. A. Robb, J. R. Cheeseman, V. G. Zakrzewski, J. A. Montgomery, Jr., R. E. Stratmann, J. C. Burant, S. Dapprich, J. M. Millam, A. D. Daniels, K. N. Kudin, M. C. Strain, O. Farkas, J. Tomasi, V. Barone, M. Cossi, R. Cammi, B. Mennucci, C. Pomelli, C. Adamo, S. Clifford, J. Ochterski, G. A. Petersson, P. Y. Ayala, Q. Cui, K. Morokuma, P. Salvador, J. J. Dannenberg, D. K. Malick, A. D. Rabuck, K. Raghavachari, J. B. Foresman, J. Cioslowski, J. V. Ortiz, A. G. Baboul, B. B. Stefanov, G.Liu, A. Liashenko, P. Piskorz, I. Komaromi, R. Gomperts, R. L. Martin, D. J. Fox, T. Keith, M. A. Al-Laham, C. Y. Peng, A. Nanayakkara, M. Challacombe, P. M. W. Gill, B. Johnson, W. Chen, M. W. Wong, J. L. Andres, C. Gonzalez, M. Head-Gordon, E. S. Replogle, J. A. Pople, Gaussian 98 – Revision A.11, Gaussian, Inc., Pittsburgh, PA, 2001.
[36] C. M. Breneman, K. B. Wiberg, Determining atom-centered monopoles from molecular electrostatic potentials – the need for high sampling density in formamide conformational-analysis, *J. Comp. Chem.* **1990**, *11*, 361 – 373.
[37] R. Todeschini, V. Consonni, A. Mauri, M. Pavan, Dragon, Web Version 3.0, Milano, Italy, 2003.
[38] R. Todeschini, P. Gramatica, 3D-modelling and prediction by WHIM descriptors. 5. Theory development and chemical meaning of WHIM descriptors, *Quant. Struc.-Act. Relat.* **1997**, *16*, 113 – 119.
[39] M. C. Hemmer, V. Steihhauer, J. Gasteiger, Deriving the 3D structure of organic molecules from their infrared spectra, *Vib. Spectrosc.* **1999**, *19*, 151 – 164.

 © 2003 WILEY-VCH Verlag GmbH & Co. KGaA, Weinheim

[40] ChemPlus: Modular Extensions to HyperChem Release 6.02, Molecular Modeling for Windows, HyperClub, Inc., Gainesville, 2000.
[41] P. C. Jurs, S. L. Dixon, L. M. Egolf, Molecular Concepts: Representations of Molecules, in: H. van de Waterbeemd (Ed.), *Chemometric Methods in Molecular Design*, VCH, New York, **1996**, pp. 15 – 38.
[42] H. Kubinyi, *QSAR: Hansch Analysis and Related Approaches*, Vol. 1, VCH, New York, **1993**, pp 100 – 107.
[43] Infometrix, Inc., Pirouette 3.01, Woodinville, WA, 2001.
[44] A. L. Spek, PLATON: A Multipurpose Crystallographic Tool, version 31000, Utrecht University, Utrecht, 2000.
[45] WebLab ViewerLite, version 4.0., Molecular Simulations, Inc., San Diego, 2000.
[46] Titan, version 1, Wavefunction, Inc., Irvine, 2000.
[47] J. Vojtechovsky, K. Chu, J. Berendzen, R. M. Sweet, I. Schlichting, Crystal structures of myoglobin-ligand complexes at near-atomic resolution, *Biophys. J.* **1999**, *74*, 2153 – 2174.
[48] T. A. Halgren, Merck molecular force field .1. Basis, form, scope, parameterization, and performance of MMFF94, *J. Comp. Chem.* **1996**, *17*, 490 – 519.
[49] S. Tonmunphean, V. Parasuk, S. Kokpol, QSAR Study of Antimalarial Activities and Artemisinin-Heme Binding Properties Obtained from Docking Calculations, *Quant. Struct.-Act. Relat.* **2000**, *19*, 475 – 483.
[50] K. A. Johnson, High Resolution X-Ray Structures of Myoglobin-and Hemoglobin-Alkyl Isocyanide Complexes, Thesis, Rice University, Houston, TX, **1993.**
[51] M. Nishio, M. Hirota, Y. Umezawa, *The CH/π Interaction*, Wiley-VCH, New York, **1998.**
[52] F. H. Allen, O. Kennard, D. G. Watson, L. Brammer, A. G. Orpen, R. Taylor, Tables of Bond Lengths determined by X-Ray and Neutron Diffraction. Part 1. Bond Lengths in Organic Compounds, *J. Chem. Soc. Perkin Trans. II* **1987**, S1 – S19.
[53] M. Jung, H. N. ElSohly, E. M. Croom, A. T. McPhail, D. R. McPhail, Practical conversion of artemisinic acid into desoxyartemisinin, *J. Org. Chem.* **1986**, *51*, 5417 – 5419.
[54] M. A. Avery, W. K. M. Chong, J. E. Bupp, Tricyclic analogs of artemisinin – synthesis and antimalarial activity of (+)-4,5-secoartemisinin and (−)-5-nor-4,5-secoartemisinin, *J. Chem. Soc. Chem. Commun.* **1990**, 1487 – 1489.
[55] A. J. Lin, L.-Q. Li, D. L. Klayman, C. F. George, J. L. Flippen-Anderson, Antimalarial Activity of New Water-Soluble Dihydroartemisinin Derivatives. 3. Aromatic Amine Analogues, *J. Med. Chem.* **1990**, *33*, 2610 – 2614.
[56] C. W. Jefford, U. Burger, P. Millasson-Schmidt, G. Bernardinelli, B. L. Robinson, W. Peters, Epiartemisinin, a remarkably poor antimalarial: Implications for the mode of action, *Helv. Chim. Acta* **2000**, *83*, 1239 – 1246.
[57] J. M. Karle, A. J. Lin, Correlation of the crystal structures of diastereomeric artemisinin derivatives with their proton NMR spectra in $CDCl_3$, *Acta Cryst.* **1995**, *B51*, 1063 – 1068.
[58] H. L. Jiang, K. X. Chen, Y. Tang, J. Z. Chen, Y. Li, Q. M. Wang, R. Y. Ji, Theoretical and cyclic voltammetry studies on antimalarial mechanism of artemisinin (Qinghaosu) derivatives, *Indian J. Chem.* **1997**, *36B*, 154 – 160.
[59] M. Eckert-Maksić, N. Novak-Doumbouya, R. Kiralj, B. Kojić-Prodić, 7-oxanorbornene cycloadducts. X-ray, molecular orbital and photoelectron spectroscopic study, *J. Chem. Soc. Perkin Trans. II* **2000**, *7*, 1483 – 1487.
[60] S. L. Griffiths, C. F. Marcos, S. Perrio, S. P. Saberi, S. E. Thomas, G. J. Tustin, A. T. Wierzchleyski, Sulfoxides and Stereochemical Control in Organometallic Chemistry, *Pure Appl. Chem.* **1994**, *66*, 1565 – 1572.
[61] A. Perjessy, P. Ertl, N. Pronayova, B. Gautheron, R. Broussier, Spectroscopic and Theoretical Evidence for a Strong Electron-Donor Effect of the Oxo Ligand in Chlorodicyclopentadienyloxoniobium(V) Complexes, *J. Organometal. Chem.* **1994**, *466*, 133 – 137.
[62] J. Ziegler, R. T. Chang, D. W. Wright, Multiple-antigenic peptides of histidine-rich protein II of Plasmodium falciparum Dendrimeric biomineralization templates, *J. Am. Chem. Soc.* **1999**, *121*, 2395 – 2400.
[63] P. J. Ellis, C. A. Appleby, J. M. Guss, W. N. Hunter, D. L. Ollis, H. C. Freeman, Structure of ferric soybean leghemoglobin a nicotinate at 2.3 Å resolution, *Acta Cryst.* **1997**, *D53*, 302 – 310.
[64] S. C. Tang, S. Koch, G. C. Papaefthymiou, S. Foner, R. B. Frankel, J. A. Ibers, R. H. Holm, Axial ligation modes in iron(III) porphyrins – models for oxidized reaction states of cytochrome-P-450 enzymes and molecular-structure of iron(-III) protoporphyrin IX dimethyl ester *para*-nitrobenzenethiolate, *J. Am. Chem. Soc.* **1976**, *98*, 2414 – 2434.
[65] C. Frazao, C. M. Soares, M. A. Carrondo, E. Pohl, Z. Dauter, K. S. Wilson, M. Hervas, J. A. Navarro, M. A. De la Rosa, G. M. Sheldrick, *Ab initio* determination of the crystal structure of cytochrome c6 and comparison with plastocyanin, *Structure* **1995**, *3*, 1159 – 1169.
[66] D. Voet, J. G. Voet, *Biochemistry*, 2nd Ed., Wiley, New York, **2000**, Chapter 9.
[67] S. Benini, A. Gonzalez, W. R. Rypniewski, K. S. Wilson, J. J. Van-Beeumen, S. Ciurli, Crystal Structure of Oxidized Bacillus Pasteuriicytochrome C(553) at 0.97-Å Resolution, *Biochemistry* **2000**, *39*, 13115 – 13126.
[68] K. L. Shukla, T. M. Gund, S. R. Meshnick, Molecular modeling studies of the artemisinin (qinghaosu) – hemin interaction: Docking between the antimalarial agent and its putative receptor, *J. Mol. Graphics Mod.* **1995**, *13*, 215 – 222.

Received on March 14, 2003; Accepted on September 11, 2003

© 2003 WILEY-VCH Verlag GmbH & Co. KGaA, Weinheim